Environmental Science & Technology

pubs.acs.org/est

Article

High Pressure Inside Nanometer-Sized Particles Influences the Rate and Products of Chemical Reactions

Matthieu Riva,* Jianfeng Sun, V. Faye McNeill, Charline Ragon, Sebastien Perrier, Yinon Rudich, Sergey A. Nizkorodov, Jianmin Chen, Frédéric Caupin, Thorsten Hoffmann,* and Christian George*

Cite This: *Environ. Sci. Technol.* 2021, 55, 7786–7793

Read Online

ACCESS | Metrics & More | Article Recommendations | Supporting Information

ABSTRACT: The composition of organic aerosol has a pivotal influence on aerosol properties such as toxicity and cloud droplet formation capability, which could affect both climate and air quality. However, a comprehensive and fundamental understanding of the chemical and physical processes that occur in nanometer-sized atmospheric particles remains a challenge that severely limits the quantification and predictive capabilities of aerosol formation pathways. Here, we investigated the effects of a fundamental and hitherto unconsidered physical property of nanoparticles—the Laplace pressure. By studying the reaction of glyoxal with ammonium sulfate, both ubiquitous and important atmospheric constituents, we show that high pressure can significantly affect the chemical processes that occur in atmospheric ultrafine particles (i.e., particles < 100 nm). Using high-resolution mass spectrometry and UV−vis spectroscopy, we demonstrated that the formation of reaction products is strongly (i.e., up to a factor of 2) slowed down under high pressures typical of atmospheric nanoparticles. A size-dependent relative rate constant is determined and numerical simulations illustrate the reduction in the production of the main glyoxal reaction products. These results established that the high pressure inside nanometer-sized aerosols must be considered as a key property that significantly impacts chemical processes that govern atmospheric aerosol growth and evolution.

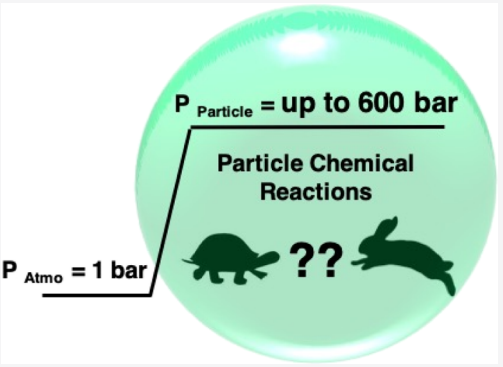

KEYWORDS: *SOA, mass spectrometry, heterogeneous chemistry, pressure, new particle formation*

INTRODUCTION

Aerosol particles are a ubiquitous component of the atmosphere, comprising small liquid and solid particles suspended in the air, with diameters that vary from a few nanometers (nm) to several tens of micrometers (μm).[1] Fine atmospheric aerosols ($PM_{2.5}$, particles with aerodynamic diameter $\leq$ 2.5 μm) produce a significant cooling effect in the atmosphere[1−3] through two mechanisms: by directly reflecting solar radiation back into space and by acting as nuclei for the formation of cloud droplets, thereby regulating cloud reflectivity and lifetime.[2,3] $PM_{2.5}$ also has a negative impact on air quality and human health, representing the fifth ranking human health risk factor globally.[4] Fine atmospheric aerosols can either be emitted directly into the air as primary aerosol or formed in the atmosphere by gas-to-particle conversion and classified as secondary aerosol.[1,5] The chemical composition of primary and secondary aerosols is mainly dominated by organic and inorganic species (and water at high relative humidity). While the inorganic species are limited to a few compounds (e.g., sulfates and nitrates are the largest contributors to submicron aerosol mass globally), there are thousands of organic compounds in aerosols.[6] The organic vapors able to grow aerosols by condensation, thus forming "secondary organic aerosol" (SOA), are primarily formed through gas-phase oxidation of volatile organic compounds (VOCs) emitted from biogenic and anthropogenic sources.[1,5] However, the precise components and physicochemical processes involved remain poorly understood. Improving our fundamental knowledge of the chemical and physical processes that govern atmospheric aerosol growth and evolution is crucial to better quantify aerosol growth and properties and hence the effect of aerosols on climate change and impact on air quality.

While research is mainly focused on elucidating the processes that control the formation and evolution of SOA, one of the most fundamental properties—the pressure inside atmospheric particles—is currently neglected in aerosol formation and growth models. The Laplace pressure is of central importance for the thermodynamic description of

Received: November 1, 2020
Revised: May 18, 2021
Accepted: May 18, 2021
Published: June 1, 2021

https://doi.org/10.1021/acs.est.0c07386
Environ. Sci. Technol. 2021, 55, 7786–7793

liquids with strongly curved interfaces (i.e., nanoparticles and nanoscale droplets). It represents the pressure difference of a droplet between the inside and outside. This effect is produced due to surface tension at the interface between a liquid and the gas interface of a curved surface.[7] The Laplace pressure is proportional to the surface tension and the inverse of the droplet size.[7] The pressure is a fundamental physical quantity that affects the values of various thermodynamic and kinetic constants of numerous chemical reactions.[8] The crucial parameters to describe the influence of pressure on chemical reactions can be further broken down, namely, the reaction volume (ΔV) and the volume of activation ($\Delta^{\ddagger}V$). The volume of activation $\Delta^{\ddagger}V$ is the volume change of the reaction system from the reactants to transition state, and the reaction volume ΔV is the corresponding volume change from the reactants to the products. The former has been studied in particular by Evans and Polanyi in their development of the transition-state theory.[9] As a result, the Laplace pressure is expected to have strong effects on the equilibrium state of any chemical system and may either accelerate or slow down a given reaction. In general, processes that lead to a net increase in the molar volume from reactants to products (i.e., $\Delta V > 0$) are thermodynamically suppressed at high pressure, and processes with a positive volume of activation from reactants to transition state are kinetically suppressed at high pressures.[10]

To investigate the influence of the internal pressure on atmospherically relevant systems, we have considered a well-studied reaction of glyoxal and ammonium sulfate. Glyoxal is among the most abundant oxygenated VOC produced in the atmosphere from the oxidation of biogenic and anthropogenic organic precursors.[11] While it was previously considered as too volatile to contribute to SOA formation, recent studies have shown that glyoxal and other small dicarbonyl species can significantly contribute to SOA growth through multiphase chemistry.[12−18] Since these species are largely produced in the gas phase, condensed-phase sinks help explaining an important part of the missing SOA mass predicted by simulations.[17,23] In the presence of ammonium sulfate, these multiphase processes produce light-absorbing complex organic compounds that contain an imidazole function.[12,19−21,24] The vast majority of the kinetic studies characterizing atmospheric chemical reactions are conducted in bulk solution[22] and/or in large aerosols;[18] hence, earlier studies on glyoxal chemistry were performed at atmospheric pressure. To demonstrate the potential importance of the internal pressure for atmospheric chemical reactions, this study has focused on the chemical characterization of glyoxal chemistry at pressures that simulate the interior of atmospheric nanoparticles (i.e., <100 nm).

EXPERIMENTAL METHODS

The experiments were performed using individual low-density polyethylene bags (VWR). Bulk samples (10 mL) were introduced into the bags that were sealed without any air. The solution mixtures contained 2 M ammonium sulfate [$(NH_4)_2SO_4$; (99.0%, Sigma-Aldrich)] and 0.25−2 M of glyoxal (40% in water, Sigma-Aldrich) corresponding to a pH of 4. Experimental conditions were selected based on earlier studies, which investigated the reaction of glyoxal with ammonium. Although these conditions do not mimic ambient concentrations, we selected this model system and reproduced the currently accepted conditions used in other studies and modified only the pressure at which the reaction took place. For each experiment, two sets of samples were prepared: (i) "control" samples were protected from ambient light and kept at room temperature and at atmospheric pressure; (ii) "pressure" samples were introduced into a high-pressure closed vessel (or reactor) and pressurized using water at 12.5, 25, or 50 MPa at room temperature (Figure S1). The five bags containing four concentrations and one control were pressurized in a high-pressure vessel (OC-1; High Pressure Equipment Company, Erie, Pennsylvania) by a piston screw pump (Top Industry, France). Once the piston reached the desired pressure, the high-pressure vessel was isolated (using valves) in order to obtain a stable pressure during the experiment. The pressure inside the vessel was continuously monitored and remained stable (i.e., less than 5% decrease over each experiment).

One set of samples comprises four solutions containing glyoxal (0.25, 0.5, 1, and 2 M) and $(NH_4)_2SO_4$ (2 M), one solution containing only glyoxal (2 M), and one water blank. The blanks were used to identify possible contamination from the bag itself. The results showed that the bags were not degraded by the chemicals (organics, acids, etc.) used in the experiments. The samples were maintained for 3, 6, 12, 18, and 24 h. At least three replicates for each condition (concentration, exposure time, and pressure) were performed.

UV−Vis Characterization. Kinetic analyses were based on measurements of the absorbance of the reaction mixtures as a function of time over 200−900 nm with a UV−vis spectrometer (Cary 60, Agilent Technology). Directly after the end of the experiments, the samples were diluted (by a factor of 10) in deionized water to stop/significantly slow down the glyoxal reaction and ensure an optimal quantification (i.e., peak absorbance < 1). The diluted reaction mixtures were taken and placed into 1 cm quartz cuvettes. Control experiments were performed (i.e., without dilution) to ensure that the dilution did not modify the composition of the reaction mixtures. The ratio of the peak absorbance of the solution at high pressure and at atmospheric pressure was similar with (e.g., ratio = 0.52, 2 M at 50 MPa) and without (ratio = 0.56; 2 M at 50 MPa) dilution. The absorption band between 260 and 300 nm was used to probe the formation of light-absorbing compounds produced from the reaction of glyoxal with ammonium ions. Note that using the analytical techniques employed in this study, it was not possible to directly monitor the reactants' concentrations. Therefore, no quantitative data on the thermodynamics were obtained.

Chemical Characterization. Solutions exposed at atmospheric pressure and at high pressures were directly diluted (×10,000) at the end of the experiments to stop the reaction. Diluted samples were analyzed by ultrahigh-performance liquid chromatography (Dionex 3000, Thermo Scientific) using a Waters Acquity HSS C18 column (1.8 μL, 100 × 2.1 mm) coupled with a Q-Exactive Hybrid Quadrupole-Orbitrap mass spectrometer (Thermo Scientific) equipped with an electrospray ionization (ESI) source operated in negative and positive modes. The mobile phase consisted of (A) 0.1% formic acid in water (Optima LC/MS, Fischer Scientific) and (B) 0.1% formic acid in acetonitrile (Optima LC/MS, Fischer Scientific). Gradient elution was carried out by the A/B mixture at a total flow rate of 300 μL/min: 1% of B for 2 min, a linear gradient was used until 100% of B for 11 min, then 100% of B for 2 min and back to 1% of B in 0.1 min, and to end 1% of B for 6.9 min. Caffeine was used as an internal standard to retrieve the ionization efficiency of the different samples in order to account for the variability of the UPLC/ESI-Orbitrap.

https://doi.org/10.1021/acs.est.0c07386
Environ. Sci. Technol. 2021, 55, 7786−7793

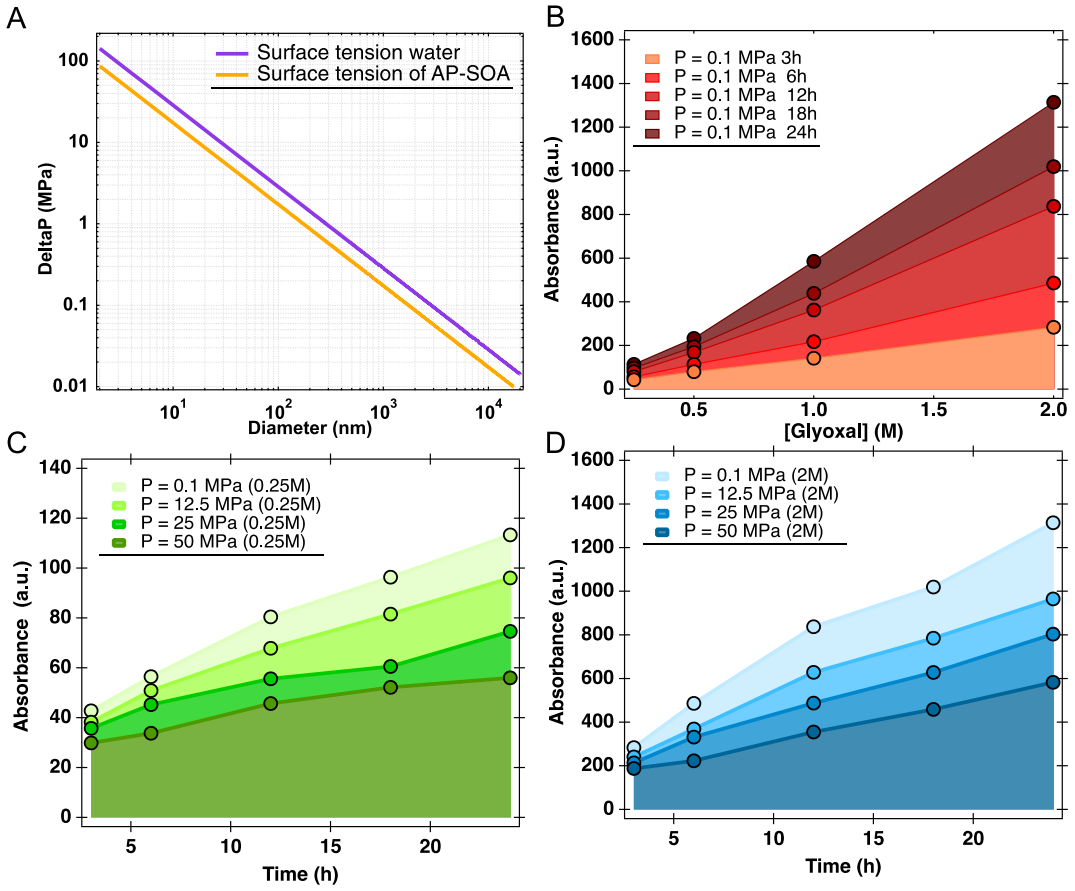

Figure 1. (A) Pressure inside 2−1000 nm aerosol particles with surface tension of water and α-pinene SOA. (B) Evolution of the absorbance (non-cumulative) of light-absorbing glyoxal reaction products at different reaction times and as a function of glyoxal concentration. Non-cumulative absorbance of light-absorbing glyoxal reaction products at different pressures of (C) 0.25 M glyoxal/2 M AS and (D) 2 M glyoxal/2 M AS as a function of reaction time.

The recovery of caffeine was 86 ± 5% (1 standard deviation), and each sample was corrected for the instrumental variability.

GAMMA Simulations. Calculations were performed using the photochemical box model GAMMA 5.0[25,26] to simulate the formation of a light-absorbing organic material in aqueous aerosols from glyoxal following Woo et al.[27] GAMMA uses a detailed kinetic treatment of glyoxal chemistry and does not assume chemical equilibrium.[25] The gas-phase concentration of glyoxal was set to 4.68×10^9 molecule cm^{-3} as previously used by Tsui et al.[26] The reaction of aqueous glyoxal with NH_4^+ to form light-absorbing organic species was simulated using the kinetics of Schwier et al.[28] for the base case and compared with simulations where that overall rate constant was reduced to account for the effects of particle pressure following the data in Figure 3. Simulations were performed for ammonium (bi)sulfate particles at 65% RH and pH 2 with a diameter of 20, 40, 80, 160, or 320 nm, with a constant liquid water content (7.25×10^{12} cm^3 cm^{-3}), and surface area density (10^{-4} cm^2 cm^{-3}). No partitioning correction was applied to take into consideration the possible Kelvin effect. In other words, to evaluate the effect of pressure, a similar aqueous-phase concentration of glyoxal was considered for the different size bins. A 12 h time period (dawn to dusk) was simulated. Ambient temperature was set to vary sinusoidally through the day with a half-period of 12 h, with the minimum temperature 298.15 K at dawn and dusk and maximum temperature 303.15 K at midday. Photochemical rate constants were set following McNeill et al.[25]

RESULTS AND DISCUSSION

Influence of Pressure on the Formation of Glyoxal Reaction Products. Assuming a liquid particle and the known surface tension (γ) (e.g., 72.74 mN m^{-1} for water and 44.4 mN m^{-1} for SOA at 20 °C),[29] the effective pressure inside nanometer-sized particles can be calculated using the Young−Laplace equation ($\Delta P = 2\gamma/r$, with r representing the radius of the particle) (Figure 1A). It should be pointed out the surface tension of nanoparticles remains basically unknown and only the surface tension of large aerosols can be determined. Hence, the surface tension of α-pinene-derived SOA and pure water was selected as lower and upper limits, respectively, to probe the impact of the pressure. Indeed, earlier studies have shown that atmospherically relevant particles, including inorganic and organic species, have surface tension within this range.[29−33] Besides surface tension, other parameters can influence the pressure, such as the phase state and/or chemical composition of the particles. For example, the surface tension of dissolved SOA from the oxidation of biogenic compounds can be reduced by a factor of 2 compared to pure water.[29] According to various studies, biogenic SOA particles produced in laboratory chambers or observed in the ambient atmosphere may exist in various solid and liquid forms.[34−36] However, nanometer-sized organic aerosols remain liquid under most

https://doi.org/10.1021/acs.est.0c07386
Environ. Sci. Technol. 2021, 55, 7786−7793

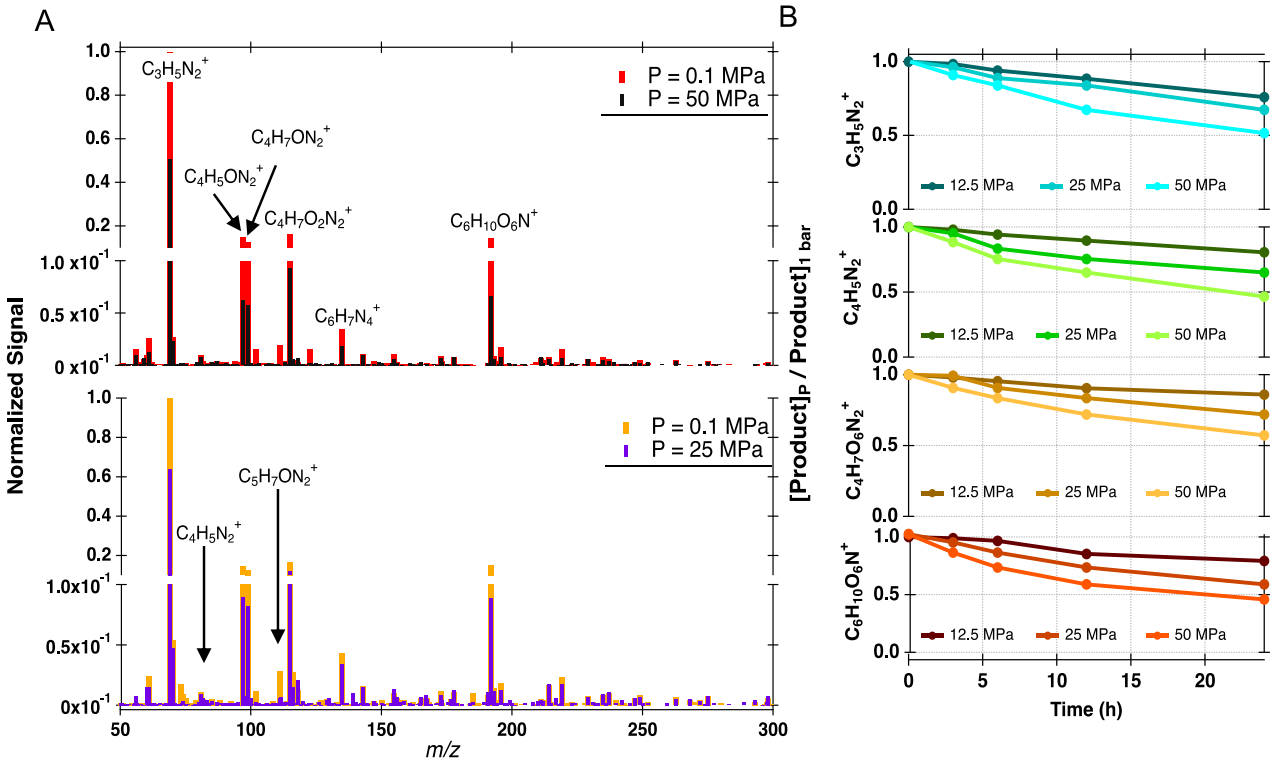

Figure 2. (A) Impact of the pressure on the chemical composition of organic products from the reaction of glyoxal with ammonium sulfate measured by UPLC-(+)ESI-Orbitrap. Mass spectra were averaged across the chromatogram and background subtracted (i.e., water samples served as blank). (B) Evolution of the relative concentration ($[\text{product}]_{P\gg 1\text{atm}}/[\text{product}]_{P=1\text{atm}}$) of the main reaction products as a function of time.

environmental conditions.[36−38] To investigate the impact of pressure on atmospheric chemical reactions that occur within the particles, we studied the reaction between glyoxal and ammonium sulfate under different pressures ranging from 1 atm to 500 atm: 0.1, 12.5, 25, and 50 MPa corresponding to coarse particles and to fine aerosol particles of 23, 12, and 6 nm diameter, respectively (diameters calculated assuming a liquid droplet with a surface tension of pure water). As previously reported, products formed from the glyoxal−ammonium sulfate reaction absorb light in the UV and visible wavelengths providing a convenient way to follow the reaction (Figures 1 and S2−S5).[19,20,39] Figure 1B shows the time evolution of the UV absorption spectra of a solution initially containing 0.25, 0.5, 1, and 2 M glyoxal mixed with 2 M of ammonium sulfate $[(NH_4)_2SO_4]$ up to 24 h, corresponding to experimental conditions conducted under atmospheric pressure (i.e., 1 atm internal pressure).[20] The resulting solution is weakly acidic (pH ∼ 4), thus simulating aqueous tropospheric aerosol particles. The absorbance of solutions at atmospheric pressure increased with time. Under high pressures, a significant decrease in the total absorbance is observed for all conditions investigated in this study (Figures 1C,D and S2). Already after 3 h, the difference between experiments conducted at atmospheric pressure and 50 MPa experiments is significant (i.e., $Abs_{P50}/Abs_{P0.1} = 0.66 \pm 0.02$), underlying the impact of increased pressure on the rate of glyoxal's reaction under slightly acidic aqueous conditions. Interestingly, related reactions between carbonyls and amines have been studied in the context of food science, and a retarding effect of high (400 MPa) pressure was demonstrated.[40−42] This observation is consistent with our results, although we find an effect on the reaction of glyoxal with ammonium sulfate at much milder pressures, for example, slowing down by a factor of 2 at 25 MPa. This proves that pressure can already have a pronounced effect in a relevant size range for atmospheric aerosols. It is important to point out that in this study, we have explored the effect of pressure in bulk solution in a closed system; that is, no partitioning was considered. As a result, the decreasing rate constant is only due to the effect of pressure on the chemical processes. Additional studies are required to relate what we observed in bulk solution to aerosol particles.

Ultrahigh-performance liquid chromatography coupled with hybrid quadrupole Orbitrap mass spectrometry analysis, performed in negative and positive modes, shows the presence of a wide variety of reaction products (Figure 2A). The major reaction products, detected by their protonated ions and consistent with other studies that form through the iminium pathway,[19,20,22,24,43] [i.e., imidazole ($C_3H_5N_2^+$), imidazole-2-carboxaldehyde ($C_4H_5ON_2^+$), and hydrated imidazole-2-carboxaldehyde ($C_4H_7O_2N_2^+$)], are observed in all the experiments. This product distribution is consistent with the existing literature, where high-molecular-weight organic compounds, formed by accretion reactions, have been observed.[12,19,20,43] Although the reaction products are similar in our study, samples exposed to high pressures exhibit much lower product yields compared to the atmospheric pressure samples (Figure 2A). More specifically, concentrations of the primary products, such as imidazole, reduced by a factor of 2 after 24 h, further highlighting the impact of pressure on this chemical system (Figure 2B). As in the Maillard reaction,[41,44] chemical processes leading to the formation of such products increase the volume of reaction (i.e., $\Delta V > 0$). Therefore, at higher pressure, the product formation is reduced. In addition, formation of N-containing oligomers is also significantly suppressed by the pressure (∼40% after 24 h). For example, the formation of $C_6H_{10}O_6N^+$ dimer is strongly reduced under

https://doi.org/10.1021/acs.est.0c07386
Environ. Sci. Technol. 2021, 55, 7786−7793

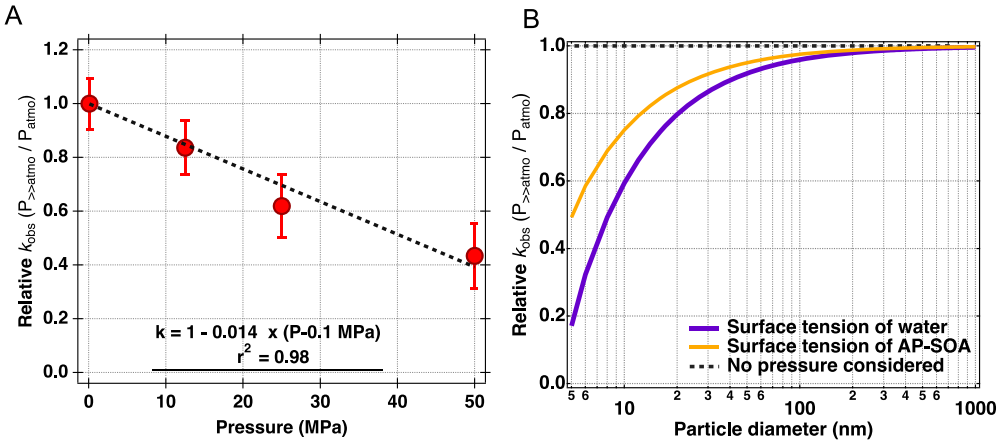

Figure 3. (A) Relative glyoxal/AS reaction rate constant of light-absorbing product formation as a function of pressure. The overall uncertainty of the relative rate constant is 0.074 (1 standard deviation). (B) Relative glyoxal/AS reaction rate constant as a function of aerosol particle diameter considering different aerosol surface tension.

high pressures (Figure 2). Finally, it is noted that the glyoxal products formed from aldol/acetal oligomerization were not observed in either the atmospheric pressure or the high-pressure samples. Overall, the results obtained in this study reveal that the Laplace pressure, that is, the pressure within atmospheric particles, can strongly influence the multiphase processes involved in the formation and growth of SOA.

Particle Size-Dependent Kinetics. As the light-absorbing compounds absorb light at 290 nm (Figure S4), monitoring the evolution of this absorbance band provides insights into the overall kinetics of the reaction between glyoxal and ammonium cations. The reactions are first order (Figure S5) within the first 24 h, which is consistent with an earlier study.[20] Therefore, for each set of experiments (i.e., four concentrations at a given pressure and four concentrations at atmospheric pressure), where each condition was repeated at least three times, a global rate constant (k_{obs}) can be obtained. As shown in Figure 3A, a pressure-dependent rate constant is determined, using the average k_{obs} determined for each pressure. Using linear regression, particle size-dependence of the rate constant can be obtained, as shown in Figure 3B. Two surface tension values were selected to obtain the rate constant as a function of particle size: the surface tension of water (72.74 mN m^{-1}), which represents an upper limit, and the surface tension of α-pinene SOA, which is formed under humid conditions (44.4 mN m^{-1}).[29] α-Pinene-derived SOA is used as model SOA because monoterpenes are among the most important SOA precursors on a global scale.[45,46] Therefore, for ultrafine particles, that is, <100 nm, the reduction of glyoxal chemistry is important, indicating that chemical processes identical or similar to those involved in the heterogeneous chemistry of the dicarbonyls can be strongly reduced in ultrafine atmospheric aerosols.

To further illustrate the particle size-dependence chemistry, the photochemical box model GAMMA was used to simulate imidazole formation as a function of particle size (and hence pressure). The calculations were performed in discrete size bins (i.e., 20, 40, 80, 160, and 320 nm) for 12 h (Figure 4).[25,27,47] The simulations show that the pressure effect on the formation of imidazole and other brown carbon species is negligible for the largest size bin (i.e., 320 nm). However, the heterogeneous process is greatly reduced when the pressure within the nanometer-sized particles increases. For example,

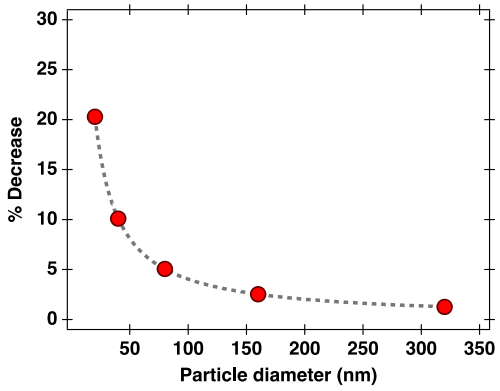

Figure 4. Decrease of the formation of glyoxal reaction products as a function of particle size diameter. Simulations were performed using GAMMA for different size bins diameters (e.g., 20, 40, 80, 160, and 320 nm) and under Eastern US rural conditions.

the formation of glyoxal reaction products is reduced by 20% for the smallest size bin (i.e., 20 nm). This further underlines that chemical processes that are expected to grow ultrafine particles[48] are likely to be strongly influenced by their high internal pressure.

By studying an important chemical reaction under relevant atmospheric conditions, we showed that the high pressure inside nanometer-sized aerosol particles is a key property that has not been considered hitherto and that can have a significant influence on the chemical processes governing atmospheric particle growth and evolution. More importantly, we demonstrated that pressures can have a noticeable effect at much milder pressures (~1−2 orders of magnitude lower) than has been studied before. Such pressures are highly relevant for atmospheric aerosols. However, it is important to note that due to the relative short lifetime of nanoparticles (i.e., from a few hours to a day), the pressure would have a noticeable effect for chemical reactions that are greatly impacted by the Laplace pressure with rate constant comparable or shorter than the aerosol lifetime. Considering the Evans−Polanyi principle, Le Noble and co-workers[49] have derived a function to represent the reaction profile for a one-step reaction. By using such an approach, it is possible to evaluate the impact of pressure on changes in the transition state. As we studied a global reaction, it was not possible to

https://doi.org/10.1021/acs.est.0c07386
Environ. Sci. Technol. 2021, 55, 7786−7793

isolate a single reaction step using the analytical techniques employed by Le Noble et al.[49] However, based on the existing literature, we can derive some information providing hints that identify which reaction step may have been mostly impacted by the pressure.[8,50] For example, the breaking of bonds within a reaction mechanism involves the separation of atoms from each other from covalent distances to van der Waals distances. In fact, the transformation of NH_4^+ to H^+ and NH_3, which was identified to be a key state of the investigated chemistry,[19,24] is known to be hindered by pressure (i.e., ΔV = 7 cm^3 mol^{-1})[50,51] and might explain the observation made here. While we found a negative effect here for this specific reaction on the formation and growth of SOA, other potentially important particle phase reactions, especially those with negative reaction volumes and/or negative activation volumes, could be strongly promoted by pressure.[1,22] The extensive literature on the effects of pressure on organic and inorganic chemical reactions in solutions strongly suggests that several types of atmospheric reactions could also be influenced by pressure.[8] For example, nucleophilic substitution reactions of various types of organic compounds at high pressure are favored because ionization reactions in the transition state of the reaction cause negative activation volumes. While the experiments performed in this work show a clear impact of the pressure, additional experiments using aerosol droplets are required to further confirm the results presented here. Indeed, interfacial chemistry, gas−liquid exchanges, that is, processes not considered here, may also be affected by the pressure in addition to the "bulk" chemical reaction kinetics and equilibria. Overall, our results provide information about the potentially critical influence of pressure on the chemistry occurring within atmospheric nanoparticles. While such processes have not been reported before, this work emphasizes the need to consider particle phase processing under atmospherically relevant conditions.

■ ASSOCIATED CONTENT

Supporting Information

The Supporting Information is available free of charge at https://pubs.acs.org/doi/10.1021/acs.est.0c07386.

Experimental device (high-pressure vessel) used in this study; absorbance of light-absorbing glyoxal oxidation products at different reaction times and pressures; relative absorbance of light-absorbing glyoxal oxidation products under the different experimental conditions used in this study; absorption spectra of glyoxal products after 24 h; and first-order kinetic fit for the different experiments performed in this study (PDF)

■ AUTHOR INFORMATION

Corresponding Authors

Matthieu Riva − *Univ. Lyon, Université Claude Bernard Lyon 1, CNRS, IRCELYON, Villeurbanne F-69626, France;* orcid.org/0000-0003-0054-4131; Email: matthieu.riva@ircelyon.univ-lyon1.fr

Thorsten Hoffmann − *Department of Chemistry, Johannes Gutenberg-Universität, Mainz 55128, Germany;* Email: t.hoffmann@uni-mainz.de

Christian George − *Univ. Lyon, Université Claude Bernard Lyon 1, CNRS, IRCELYON, Villeurbanne F-69626, France;* orcid.org/0000-0003-1578-7056; Email: christian.george@ircelyon.univ-lyon1.fr

Authors

Jianfeng Sun − *Univ. Lyon, Université Claude Bernard Lyon 1, CNRS, IRCELYON, Villeurbanne F-69626, France; Shanghai Key Laboratory of Atmospheric Particle Pollution and Prevention (LAP3), Department of Environmental Science & Engineering, Fudan University, Shanghai 200433, China*

V. Faye McNeill − *Department of Chemical Engineering and Department of Earth and Environmental Sciences, Columbia University, New York 10025, United States;* orcid.org/0000-0003-0379-6916

Charline Ragon − *Univ. Lyon, Université Claude Bernard Lyon 1, CNRS, IRCELYON, Villeurbanne F-69626, France*

Sebastien Perrier − *Univ. Lyon, Université Claude Bernard Lyon 1, CNRS, IRCELYON, Villeurbanne F-69626, France*

Yinon Rudich − *Department of Earth and Planetary Sciences, Weizmann Institute, Rehovot 76100, Israel;* orcid.org/0000-0003-3149-0201

Sergey A. Nizkorodov − *Department of Chemistry, University of California, Irvine 92697, California, United States;* orcid.org/0000-0003-0891-0052

Jianmin Chen − *Shanghai Key Laboratory of Atmospheric Particle Pollution and Prevention (LAP3), Department of Environmental Science & Engineering, Fudan University, Shanghai 200433, China;* orcid.org/0000-0001-5859-3070

Frédéric Caupin − *Université de Lyon, Université Claude Bernard Lyon 1, CNRS, Institut Lumière Matière, Villeurbanne F-69622, France;* orcid.org/0000-0002-8892-2514

Complete contact information is available at: https://pubs.acs.org/10.1021/acs.est.0c07386

Notes

The authors declare no competing financial interest.

■ ACKNOWLEDGMENTS

The authors would like to thank the European Research Council (ERC-StG), the Deutsche Forschungsgemeinschaft, and the University of Lyon for financial support. S.A.N. thanks the Université Claude Bernard Lyon 1 for providing him with a visiting professorship in the summer of 2018.

■ REFERENCES

(1) Hallquist, M.; Wenger, J. C.; Baltensperger, U.; Rudich, Y.; Simpson, D.; Claeys, M.; Dommen, J.; Donahue, N. M.; George, C.; Goldstein, A. H.; Hamilton, J. F.; Herrmann, H.; Hoffmann, T.; Iinuma, Y.; Jang, M.; Jenkin, M. E.; Jimenez, J. L.; Kiendler-Scharr, A.; Maenhaut, W.; McFiggans, G.; Mentel, T. F.; Monod, A.; Prévôt, A. S. H.; Seinfeld, J. H.; Surratt, J. D.; Szmigielski, R.; Wildt, J. The Formation, Properties and Impact of Secondary Organic Aerosol: Current and Emerging Issues. *Atmos. Chem. Phys.* **2009**, *9*, 5155−5236.

(2) Albrecht, B. A. Aerosols, Cloud Microphysics, and Fractional Cloudiness. *Science* **1989**, *245*, 1227−1230.

(3) Twomey, S. The Influence of Pollution on the Shortwave Albedo of Clouds. *J. Atmos. Sci.* **1977**, *34*, 1149−1152.

(4) Gakidou, E.; Afshin, A.; Abajobir, A. A.; Abate, K. H.; Abbafati, C.; Abbas, K. M.; Abd-Allah, F.; Abdulle, A. M.; Abera, S. F.; Aboyans, V.; et al. Global, Regional, and National Comparative Risk Assessment of 84 Behavioural, Environmental and Occupational, and Metabolic Risks or Clusters of Risks, 1990−2016: A Systematic Analysis for the Global Burden of Disease Study 2016. *Lancet* **2017**, *390*, 1345−1422.

(5) Shrivastava, M.; Cappa, C. D.; Fan, J.; Goldstein, A. H.; Guenther, A. B.; Jimenez, J. L.; Kuang, C.; Laskin, A.; Martin, S. T.; Ng, N. L.; Petaja, T.; Pierce, J. R.; Rasch, P. J.; Roldin, P.; Seinfeld, J. H.; Shilling, J.; Smith, J. N.; Thornton, J. A.; Volkamer, R.; Wang, J.; Worsnop, D. R.; Zaveri, R. A.; Zelenyuk, A.; Zhang, Q. Recent Advances in Understanding Secondary Organic Aerosol: Implications for Global Climate Forcing: Advances in Secondary Organic Aerosol. *Rev. Geophys.* **2017**, *55*, 509−559.
(6) Jimenez, J. L.; Canagaratna, M. R.; Donahue, N. M.; Prevot, A. S. H.; Zhang, Q.; Kroll, J. H.; DeCarlo, P. F.; Allan, J. D.; Coe, H.; Ng, N. L.; Aiken, A. C.; Docherty, K. S.; Ulbrich, I. M.; Grieshop, A. P.; Robinson, A. L.; Duplissy, J.; Smith, J. D.; Wilson, K. R.; Lanz, V. A.; Hueglin, C.; Sun, Y. L.; Tian, J.; Laaksonen, A.; Raatikainen, T.; Rautiainen, J.; Vaattovaara, P.; Ehn, M.; Kulmala, M.; Tomlinson, J. M.; Collins, D. R.; Cubison, M. J.; Dunlea, E. J.; Huffman, J. A.; Onasch, T. B.; Alfarra, M. R.; Williams, P. I.; Bower, K.; Kondo, Y.; Schneider, J.; Drewnick, F.; Borrmann, S.; Weimer, S.; Demerjian, K.; Salcedo, D.; Cottrell, L.; Griffin, R.; Takami, A.; Miyoshi, T.; Hatakeyama, S.; Shimono, A.; Sun, J. Y.; Zhang, Y. M.; Dzepina, K.; Kimmel, J. R.; Sueper, D.; Jayne, J. T.; Herndon, S. C.; Trimborn, A. M.; Williams, L. R.; Wood, E. C.; Middlebrook, A. M.; Kolb, C. E.; Baltensperger, U.; Worsnop, D. R. Evolution of Organic Aerosols in the Atmosphere. *Science* **2009**, *326*, 1525−1529.
(7) Ibach, H. *Physics of Surfaces and Interfaces*; Springer: Berlin; New York, 2006.
(8) Drljaca, A.; Hubbard, C. D.; van Eldik, R.; Asano, T.; Basilevsky, M. V.; le Noble, W. J. Activation and Reaction Volumes in Solution. 3. *Chem. Rev.* **1998**, *98*, 2167−2290.
(9) Laidler, K. J.; King, M. C. Development of Transition-State Theory. *J. Phys. Chem.* **1983**, *87*, 2657−2664.
(10) Chen, B.; Hoffmann, R.; Cammi, R. The Effect of Pressure on Organic Reactions in Fluids-a New Theoretical Perspective. *Angew. Chem., Int. Ed.* **2017**, *56*, 11126−11142.
(11) Fu, T.-M.; Jacob, D. J.; Wittrock, F.; Burrows, J. P.; Vrekoussis, M.; Henze, D. K. Global Budgets of Atmospheric Glyoxal and Methylglyoxal, and Implications for Formation of Secondary Organic Aerosols. *J. Geophys. Res.* **2008**, *113*, D15303.
(12) Galloway, M. M.; Chhabra, P. S.; Chan, A. W. H.; Surratt, J. D.; Flagan, R. C.; Seinfeld, J. H.; Keutsch, F. N. Glyoxal Uptake on Ammonium Sulphate Seed Aerosol: Reaction Products and Reversibility of Uptake under Dark and Irradiated Conditions. *Atmos. Chem. Phys.* **2009**, *9*, 3331−3345.
(13) Liggio, J. Reactive Uptake of Glyoxal by Particulate Matter. *J. Geophys. Res.* **2005**, *110*, D10304.
(14) Kroll, J. H.; Ng, N. L.; Murphy, S. M.; Varutbangkul, V.; Flagan, R. C.; Seinfeld, J. H. Chamber Studies of Secondary Organic Aerosol Growth by Reactive Uptake of Simple Carbonyl Compounds. *J. Geophys. Res.* **2005**, *110*, D23207.
(15) Corrigan, A. L.; Hanley, S. W.; De Haan, D. O. Uptake of Glyoxal by Organic and Inorganic Aerosol. *Environ. Sci. Technol.* **2008**, *42*, 4428−4433.
(16) Haan, D. O. D.; Corrigan, A. L.; Smith, K. W.; Stroik, D. R.; Turley, J. J.; Lee, F. E.; Tolbert, M. A.; Jimenez, J. L.; Cordova, K. E.; Ferrell, G. R. Secondary Organic Aerosol-Forming Reactions of Glyoxal with Amino Acids. *Environ. Sci. Technol.* **2009**, *43*, 2818−2824.
(17) Ervens, B.; Volkamer, R. Glyoxal Processing by Aerosol Multiphase Chemistry: Towards a Kinetic Modeling Framework of Secondary Organic Aerosol Formation in Aqueous Particles. *Atmos. Chem. Phys.* **2010**, *10*, 8219−8244.
(18) Trainic, M.; Abo Riziq, A.; Lavi, A.; Flores, J. M.; Rudich, Y. The Optical, Physical and Chemical Properties of the Products of Glyoxal Uptake on Ammonium Sulfate Seed Aerosols. *Atmos. Chem. Phys.* **2011**, *11*, 9697−9707.
(19) Yu, G.; Bayer, A. R.; Galloway, M. M.; Korshavn, K. J.; Fry, C. G.; Keutsch, F. N. Glyoxal in Aqueous Ammonium Sulfate Solutions: Products, Kinetics and Hydration Effects. *Environ. Sci. Technol.* **2011**, *45*, 6336−6342.
(20) Nozière, B.; Dziedzic, P.; Córdova, A. Products and Kinetics of the Liquid-Phase Reaction of Glyoxal Catalyzed by Ammonium Ions (NH_4^+). *J. Phys. Chem. A* **2009**, *113*, 231−237.
(21) Rossignol, S.; Aregahegn, K. Z.; Tinel, L.; Fine, L.; Nozière, B.; George, C. Glyoxal Induced Atmospheric Photosensitized Chemistry Leading to Organic Aerosol Growth. *Environ. Sci. Technol.* **2014**, *48*, 3218−3227.
(22) Herrmann, H.; Schaefer, T.; Tilgner, A.; Styler, S. A.; Weller, C.; Teich, M.; Otto, T. Tropospheric Aqueous-Phase Chemistry: Kinetics, Mechanisms, and Its Coupling to a Changing Gas Phase. *Chem. Rev.* **2015**, *115*, 4259−4334.
(23) Volkamer, R.; San Martini, F.; Molina, L. T.; Salcedo, D.; Jimenez, J. L.; Molina, M. J. A Missing Sink for Gas-Phase Glyoxal in Mexico City: Formation of Secondary Organic Aerosol. *Geophys. Res. Lett.* **2007**, *34*, L19807.
(24) Kampf, C. J.; Jakob, R.; Hoffmann, T. Identification and Characterization of Aging Products in the Glyoxal/Ammonium Sulfate System—Implications for Light-Absorbing Material in Atmospheric Aerosols. *Atmos. Chem. Phys.* **2012**, *12*, 6323−6333.
(25) McNeill, V. F.; Woo, J. L.; Kim, D. D.; Schwier, A. N.; Wannell, N. J.; Sumner, A. J.; Barakat, J. M. Aqueous-Phase Secondary Organic Aerosol and Organosulfate Formation in Atmospheric Aerosols: A Modeling Study. *Environ. Sci. Technol.* **2012**, *46*, 8075−8081.
(26) Tsui, W. G.; Woo, J. L.; McNeill, V. F. Impact of Aerosol-Cloud Cycling on Aqueous Secondary Organic Aerosol Formation. *Atmosphere* **2019**, *10*, 666.
(27) Woo, J. L.; Kim, D. D.; Schwier, A. N.; Li, R.; McNeill, V. F. Aqueous Aerosol SOA Formation: Impact on Aerosol Physical Properties. *Faraday Discuss.* **2013**, *165*, 357.
(28) Schwier, A. N.; Sareen, N.; Mitroo, D.; Shapiro, E. L.; McNeill, V. F. Glyoxal-Methylglyoxal Cross-Reactions in Secondary Organic Aerosol Formation. *Environ. Sci. Technol.* **2010**, *44*, 6174−6182.
(29) Hritz, A. D.; Raymond, T. M.; Dutcher, D. D. A Method for the Direct Measurement of Surface Tension of Collected Atmospherically Relevant Aerosol Particles Using Atomic Force Microscopy. *Atmos. Chem. Phys.* **2016**, *16*, 9761−9769.
(30) Bzdek, B. R.; Power, R. M.; Simpson, S. H.; Reid, J. P.; Royall, C. P. Precise, Contactless Measurements of the Surface Tension of Picolitre Aerosol Droplets. *Chem. Sci.* **2016**, *7*, 274−285.
(31) Gray Bé, A.; Upshur, M. A.; Liu, P.; Martin, S. T.; Geiger, F. M.; Thomson, R. J. Cloud Activation Potentials for Atmospheric α-Pinene and β-Caryophyllene Ozonolysis Products. *ACS Cent. Sci.* **2017**, *3*, 715−725.
(32) Schwier, A. N.; Viglione, G. A.; Li, Z.; Faye McNeill, V. Modeling the Surface Tension of Complex, Reactive Organic−Inorganic Mixtures. *Atmos. Chem. Phys.* **2013**, *13*, 10721−10732.
(33) Shapiro, E. L.; Szprengiel, J.; Sareen, N.; Jen, C. N.; Giordano, M. R.; McNeill, V. F. Light-Absorbing Secondary Organic Material Formed by Glyoxal in Aqueous Aerosol Mimics. *Atmos. Chem. Phys.* **2009**, *9*, 2289−2300.
(34) Bateman, A. P.; Gong, Z.; Liu, P.; Sato, B.; Cirino, G.; Zhang, Y.; Artaxo, P.; Bertram, A. K.; Manzi, A. O.; Rizzo, L. V.; Souza, R. A. F.; Zaveri, R. A.; Martin, S. T. Sub-Micrometre Particulate Matter Is Primarily in Liquid Form over Amazon Rainforest. *Nat. Geosci.* **2016**, *9*, 34−37.
(35) Cappa, C. D.; Wilson, K. R. Evolution of Organic Aerosol Mass Spectra upon Heating: Implications for OA Phase and Partitioning Behavior. *Atmos. Chem. Phys.* **2011**, *11*, 1895−1911.
(36) Virtanen, A.; Joutsensaari, J.; Koop, T.; Kannosto, J.; Yli-Pirilä, P.; Leskinen, J.; Mäkelä, J. M.; Holopainen, J. K.; Pöschl, U.; Kulmala, M.; Worsnop, D. R.; Laaksonen, A. An Amorphous Solid State of Biogenic Secondary Organic Aerosol Particles. *Nature* **2010**, *467*, 824−827.
(37) Cheng, Y.; Su, H.; Koop, T.; Mikhailov, E.; Pöschl, U. Size Dependence of Phase Transitions in Aerosol Nanoparticles. *Nat. Commun.* **2015**, *6*, 5923.
(38) Virtanen, A.; Kannosto, J.; Kuuluvainen, H.; Arffman, A.; Joutsensaari, J.; Saukko, E.; Hao, L.; Yli-Pirilä, P.; Tiitta, P.; Holopainen, J. K.; Keskinen, J.; Worsnop, D. R.; Smith, J. N.;

https://doi.org/10.1021/acs.est.0c07386
Environ. Sci. Technol. 2021, 55, 7786−7793

Laaksonen, A. Bounce Behavior of Freshly Nucleated Biogenic Secondary Organic Aerosol Particles. *Atmos. Chem. Phys.* **2011**, *11*, 8759−8766.
(39) Powelson, M. H.; Espelien, B. M.; Hawkins, L. N.; Galloway, M. M.; De Haan, D. O. Brown Carbon Formation by Aqueous-Phase Carbonyl Compound Reactions with Amines and Ammonium Sulfate. *Environ. Sci. Technol.* **2014**, *48*, 985−993.
(40) De Vleeschouwer, K.; Van der Plancken, I.; Van Loey, A.; Hendrickx, M. E. The Effect of High Pressure−High Temperature Processing Conditions on Acrylamide Formation and Other Maillard Reaction Compounds. *J. Agric. Food Chem.* **2010**, *58*, 11740−11748.
(41) Moreno, F. J.; Molina, E.; Olano, A.; López-Fandiño, R. High-Pressure Effects on Maillard Reaction between Glucose and Lysine. *J. Agric. Food Chem.* **2003**, *51*, 394−400.
(42) Schwarzenbolz, U.; Förster, A.; Henle, T. Influence of High Hydrostatic Pressure on the Reaction between Glyoxal and Lysine Residues. *Eur. Food Res. Technol.* **2017**, *243*, 1355−1361.
(43) Hamilton, J. F.; Baeza-Romero, M. T.; Finessi, E.; Rickard, A. R.; Healy, R. M.; Peppe, S.; Adams, T. J.; Daniels, M. J. S.; Ball, S. M.; Goodall, I. C. A.; Monks, P. S.; Borrás, E.; Muñoz, A. Online and Offline Mass Spectrometric Study of the Impact of Oxidation and Ageing on Glyoxal Chemistry and Uptake onto Ammonium Sulfate Aerosols. *Faraday Discuss.* **2013**, *165*, 447.
(44) Hawkins, L. N.; Lemire, A. N.; Galloway, M. M.; Corrigan, A. L.; Turley, J. J.; Espelien, B. M.; De Haan, D. O. Maillard Chemistry in Clouds and Aqueous Aerosol As a Source of Atmospheric Humic-Like Substances. *Environ. Sci. Technol.* **2016**, *50*, 7443−7452.
(45) Jokinen, T.; Berndt, T.; Makkonen, R.; Kerminen, V.-M.; Junninen, H.; Paasonen, P.; Stratmann, F.; Herrmann, H.; Guenther, A. B.; Worsnop, D. R.; Kulmala, M.; Ehn, M.; Sipilä, M. Production of Extremely Low Volatile Organic Compounds from Biogenic Emissions: Measured Yields and Atmospheric Implications. *Proc. Natl. Acad. Sci. U.S.A.* **2015**, *112*, 7123−7128.
(46) Kelly, J. M.; Doherty, R. M.; O'Connor, F. M.; Mann, G. W.; Mann, G. W. The Impact of Biogenic, Anthropogenic, and Biomass Burning Volatile Organic Compound Emissions on Regional and Seasonal Variations in Secondary Organic Aerosol. *Atmos. Chem. Phys.* **2018**, *18*, 7393−7422.
(47) Woo, J. L.; McNeill, V. F. SimpleGAMMA v1.0—a Reduced Model of Secondary Organic Aerosol Formation in the Aqueous Aerosol Phase (AaSOA). *Geosci. Model Dev.* **2015**, *8*, 1821−1829.
(48) Apsokardu, M. J.; Johnston, M. V. Nanoparticle Growth by Particle-Phase Chemistry. *Atmos. Chem. Phys.* **2018**, *18*, 1895−1907.
(49) Le Noble, W. J.; Miller, A. R.; Hamann, S. D. A Simple, Empirical Function Describing the Reaction Profile, and Some Applications. *J. Org. Chem.* **1977**, *42*, 338−342.
(50) Asano, T.; Le Noble, W. J. Activation and Reaction Volumes in Solution. *Chem. Rev.* **1978**, *78*, 407−489.
(51) Stokes, R. The Apparent Molar Volumes of Aqueous Ammonia, Ammonium Chloride, Aniline and Anilinium Chloride at 25°C and the Volume Changes on Ionization. *Aust. J. Chem.* **1975**, *28*, 2109.

https://doi.org/10.1021/acs.est.0c07386
Environ. Sci. Technol. 2021, 55, 7786−7793